Formation Mechanism of $H_2Ti_3O_7$ Nanotubes

S. Zhang,[1] L.-M. Peng,[1,2,*] Q. Chen,[1] G. H. Du,[2] G. Dawson,[3] and W. Z. Zhou[3]

[1]*Department of Electronics, Peking University, Beijing 100871, China*

[2]*Beijing Laboratory of Electron Microscopy, Institute of Physics and Center for Condensed Matter Physics, Chinese Academy of Sciences, P.O.Box 2724, Beijing 100080, China*

[3]*School of Chemistry, University of St. Andrew, St. Andrews KY16 9ST, United Kingdom*

(Received 17 July 2003; published 19 December 2003)

Formation mechanism of $H_2Ti_3O_7$ nanotubes by single-step reaction of crystalline TiO_2 and NaOH has been investigated via transmission electron microscopy examinations of series specimens with different reaction times and extensive *ab initio* calculations. It was found that the growth mechanism includes several steps. Crystalline TiO_2 reacts with NaOH, forming a highly disordered phase, which recrystallized into some $H_2Ti_3O_7$ thin plates. H-deficiency on the top surface leads to an asymmetrical environment for the surface $Ti_3O_7^{2-}$ layer. The calculations of the surface tension, elastic strain energy, interlayer coupling energy, and Coulomb force indicated that the asymmetrical environment is the principal driving force of the cleavage of the single sheets of $H_2Ti_3O_7$ from the plates and the formation of the multiwall spiral nanotubes.

DOI: 10.1103/PhysRevLett.91.256103 PACS numbers: 68.37.Lp, 61.46.+w, 77.84.Dy

While the catalytical growth of carbon nanotubes (CNTs) [1] has been well studied [2], the formation of inorganic nanotubular materials [3] in solution is a far less understood subject. A crystalline nanotube normally has a lower energy than its flat counterpart, resulting from either eliminating the dangling bonds at the edge of a finite crystal sheet, e.g., CNT [4], or reducing surface tension of a strained surface layer once it is freed from the layers beneath [5]. The former mechanism requires a nonequilibrium and high temperature environment, and in the latter case, the structure of the layer is often asymmetric [6].

$H_2Ti_3O_7$-type nanotubes can be synthesized by one-step reaction of any crystalline TiO_2 with concentrated NaOH at 130 °C [7]. In a typical experiment TiO_2 powder with particle sizes from 80 to 200 nm was added in a 10 M NaOH aqueous solution. The specimen was transferred into a sealed Teflon container and statically heated in a furnace at 130 °C for 72 h for producing high quality nanotubes. The white powder product was filtered and washed with deionized water at room temperature until *p*H reached about 7. The composition and the structure of the products were determined by several techniques including x-ray diffraction, transmission electron microscopy (TEM), energy dispersive x-ray microanalysis, and electron energy loss spectroscopy. The material has high potential applications in Li battery if the intershell protons are replaced by Li^+ and in fuel cells when high proton conductivity can be achieved. However, the formation mechanism of these nanotubes is still unknown. In this Letter we report a TEM and *ab initio* study on the formation of $H_2Ti_3O_7$ nanotubes in a near equilibrium environment. We discovered from detailed TEM studies that the nanotubes formed from peeling single trititanate sheets from some thin plates. First-principle calculations indicated that an asymmetric chemical environment may help to break the structural symmetry and introduce strain driving the peeling process and the formation of the nanotubes.

To fathom the intermediate phases during the reaction, we stopped the reaction every 2 h with other experimental conditions unchanged, and examined the specimens by TEM. It was found that in the early stage, e.g., a few hours to 24 h, TiO_2 reacted with NaOH to form a highly disordered phase, which is similar to that first observed by Kasuga *et al.* [8]. What was fascinating observed in the present work was that this disordered phase recrystallised into thin plates. The structure of these plates with only a few layers in thickness was determined by high resolution TEM (HRTEM) to be $H_2Ti_3O_7$. Investigation on the intermediate products revealed that many plates coexisted with the nanotubes. After 3 d of reaction all the plates had changed to nanotubes with a yield >90% [Fig. 1(b)].

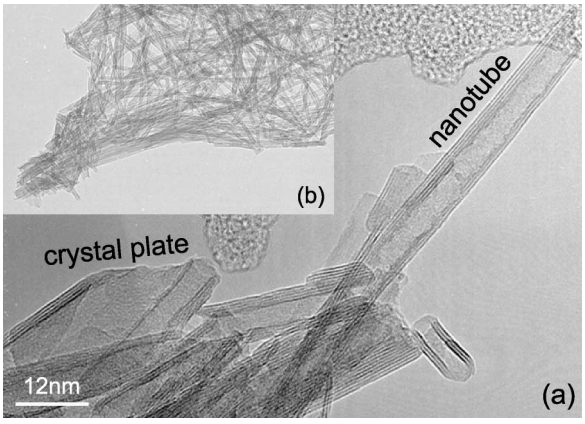

FIG. 1. (a) HRTEM image showing $H_2Ti_3O_7$ plates coexist with nanotubes after reaction of TiO_2 with NaOH for 24 h. The inset (b) shows a low-magnification TEM image of the nanotubes after the reaction for three days.

Narrow distributions of the average diameter (~7 nm) and the number of shells (~4) of the nanotubes were revealed based on examination of more than 300 nanotubes, strongly suggesting that there exists a natural mechanism for the selection of these two parameters. Detailed HRTEM examination of the nanotubes also shows that almost all nanotubes have their tube axis along the [010] direction, i.e., these nanotubes are highly symmetric achiral nanotubes.

Since TEM gave infallible evidence that the nanotubes were formed from thin plates, it becomes crucial to understand the driving force that makes this process possible. Multilayer plates of $H_2Ti_3O_7$ cannot scroll up into nanotubes since they are too rigid and, indeed, all the nanotubes we observed were made by monolayer sheets that must be peeled off from the plates. To understand the effects of chemical environments on the surface of a $Ti_3O_7^{2-}$ layer extensive *ab initio* calculations were performed for $H_2Ti_3O_7$ structures. These calculations are based on the density function theory (DFT) and performed using the CASTEP computer code [9] implemented in Cerius 2 software [10] and ultrasoft pseudopotentials [11]. The cutoff of the plane wave basis was set at 300 eV. Exchange and correlation effects were included through the generalized gradient approximation [12], and the Brillouin zone of the unit cell was sampled via a $3 \times 7 \times 3$ mesh [13]. The validity of the cutoff energy and mesh density was inferred from test calculations on anatase phase TiO_2 crystal. For this structure we obtained lattice constants $a = 0.380$ nm and $c = 0.989$ nm, in an excellent agreement with experimental values [14] and recent first-principles FLAPW calculations [15].

$Na_2Ti_3O_7$ and $H_2Ti_3O_7$ are two closely related structures. The structure of $Na_2Ti_3O_7$ was determined by Andersson and Wadsley [16], and the Ti-O framework of $D_2Ti_3O_7$ was given by Feist and Davis [17]. However, hydrogen ion positions were never published. To obtain the atomic coordinates of these titanates we have performed accurate *ab initio* structure optimization using CASTEP starting from the models of Andersson and Wadsley [16] and found that there exist several different hydrogen configurations having different total energy [18]. For the ground state with the lowest energy the structure has a space group P21/M(11), and corresponding lattice parameters are $a = 8.998$ Å, $b = 3.764$ Å, $c = 9.545$ Å, $\beta = 102.65°$ [18].

For nanotube calculations involving nearly 100 atoms, self-consistent calculations are difficult to converge with CASTEP method for configurations far away from the ground state. FastStructure code in Cerius 2 software [10] was used to optimize the atomic configurations and to calculate the total energy values. FastStructure is an *ab initio* software package specifically designed to determine the structures of molecules, solids, and surfaces by calculating the energy and forces acting on the nuclei and determining the nuclear locations corresponding to the energy minimum. FastStructure is fast in comparison with other *ab initio* methods and yields results of comparable accuracy to these methods. It achieves its speed via algorithmic improvements (e.g., making use of the so-called Harris functional [19] and a novel optimization technique) and not via parametrization. The calculations used the local-density approximation [20] for the exchange-correlation potential and an energy cutoff of 300 eV.

Although a $H_2Ti_3O_7$ layer in the bulk crystals is symmetric on both sides, the chemical environments on the two sides of a surface layer are different. As shown in Fig. 2, the negative charge of the $Ti_3O_7^{2-}$ layer on the side underneath the surface is neutralized by H^+ in the interlayer space. The H^+ on the top surface, on the other hand, may undergo frequent collision by OH^- from the solution, and the corresponding energy gain for the formation of a H_2O molecule is very large, ~2 eV. Accurate *ab initio* calculations revealed that releasing surface H may lead to some degree of contraction in the relevant Ti-O bonds on the top surface. Hydrogen deficiency on the surface therefore introduces surface tension that has a tendency for the surface layer to bend. When the average number of hydrogen loss per formula unit (δ) approaches 1, the energy associated with the surface tension becomes larger than the coupling energy between the adjacent layers (0.24 eV per formula unit). Consequently,

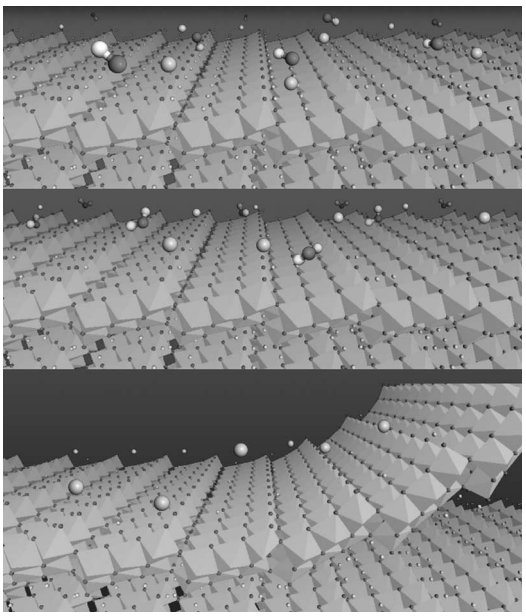

FIG. 2. Schematic models showing the effect of the alkali environment and the cleavage of the surface layer due to hydrogen deficiency on the surface. White balls: H; black balls: O; gray balls: Na. (a) A near stoichiometric $H_2Ti_3O_7$ surface in contact with many OH^- and Na^+ ions. (b) Many H^+ on the surface have been carried away by OH^-, forming H_2O. (c) When the surface hydrogen loss exceeds a critical value the surface strain energy becomes so large that the surface layer may overcome the coupling with the beneath layer and peel off from the plate.

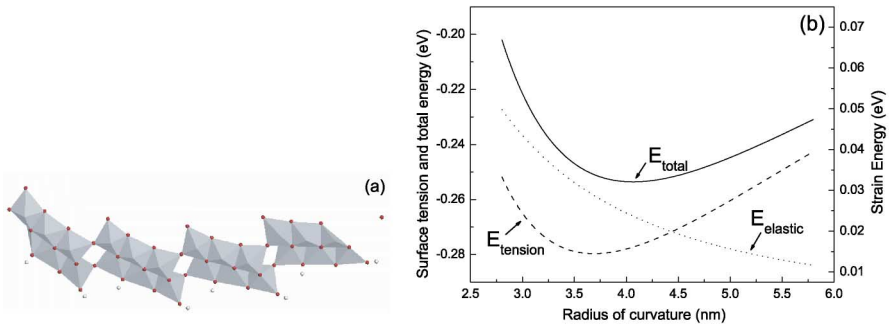

FIG. 3 (color online). (a) A relaxed curved fragment of a layer of $H_{2-\delta}Ti_3O_7$ crystal with $\delta = 1.0$. The radius of curvature of the $H_{2-\delta}Ti_3O_7$ fragment is $R = 4.16$ nm. (b) First-principle calculations of different forms of energy (per molecule) contributing to the curvature of a single trititanate sheet.

the surface layer of $H_2Ti_3O_7$ may be peeled off, most likely starting at the edge, from the surface of the plates.

A curved fragment of $H_{2-\delta}Ti_3O_7$ layer was constructed and the total energy of this fragment was calculated as a function of the radius of curvature R. Shown in Fig. 3(a) is such a relaxed fragment with $\delta = 1.0$ and $R = 4.16$ nm, where all H adsorbed on the surface side was assumed to have been taken away by OH^- ions in the NaOH solution. Electric neutrality of the hydrogen deficient $H_{2-\delta}Ti_3O_7$ layer was maintained by Na^+ ions near the surface region and, unlike H^+, these Na^+ ions were only weakly bonded to the surface. The fragment used in our calculations was composed of eight molecules of $H_{2-\delta}Ti_3O_7$. All electrons were included in the Fast-Sructure *ab initio* calculations with the maximum step size of relaxation calculation being set at 0.01 Bohr to obtain the metastable equilibrium position to preserve the curvature of the initial configuration. The geometry optimization calculation was terminated when forces on all atoms were smaller than 0.001 Ha/Bohr. Although in our model the dangling bonds at the edges of the finite fragment are not saturated as in the case of a CNT and noticeably increase the total energy of the fragment, these dangling bonds affect mainly the local bond geometry and introduce distortions toward the edges of the fragment. These distortions are basically the same for different fragments with different curvatures and hardly affect our results regarding the dependence of the total energy on the radius of curvature.

It can be shown that to a reasonable approximation we may write the total energy of a single trititanate layer as [18]

$$E_{\text{total}} = E_{\text{elastic}} + E_{\text{tension}} + E_0 = \frac{a}{R^2} + b\delta\left(\frac{\cos\theta}{R} - \frac{\delta}{R_0}\right)^2 + E_0, \quad (1)$$

where θ is the chiral angle [defined in Fig. 4(a)] and a, b, R_0 are constants, E_0 denotes the total energy of a perfect flat trititanate layer. The first energy term E_{elastic} denotes the usual elastic strain energy of a bent crystalline plate which (as in the case of a carbon nanotube) has a form $E_{\text{elastic}} \propto 1/R^2$. Numerically the $E_{\text{elastic}}(R)$ curve in Fig. 3(b) was calculated for a curved fragment like the one shown in Fig. 3(a) but with $\delta = 0$, i.e., $E_{\text{elastic}}(R) = E_{\text{total}}(R, \delta = 0)$. The second term E_{tension} is associated with the surface tension resulting from the unequalness of the H contents on the two sides of the surface layer. The $E_{\text{tension}}(R)$ curve of Fig. 3(b) corresponds to $\delta = 1$. By fitting the energy curves of Fig. 3(b) using the functional form (1) we may obtain the relevant constants a, b, R_0 and the total energy E_{total} as a function of δ. Equation (1) shows that the energy of a flat surface layer with $R = \infty$ will increase when the H^+ ions adsorbed on the surface are carried away by OH^-. We expect that the surface layer of a $H_2Ti_3O_7$ crystal plate will begin to break away from the beneath bulk layers when the coupling between them can no longer offset the energy increase due to the hydrogen deficiency on the surface. Since the coupling energy E_{coupl} is not sensitive to δ we may use $E_{\text{coupl}} = 0.24$ eV as for a perfect $H_2Ti_3O_7$ crystal plate to obtain a critical value of $\delta = 0.95$ for the peeling of the surface layer from a $H_2Ti_3O_7$ plate. Consequently the radius of the

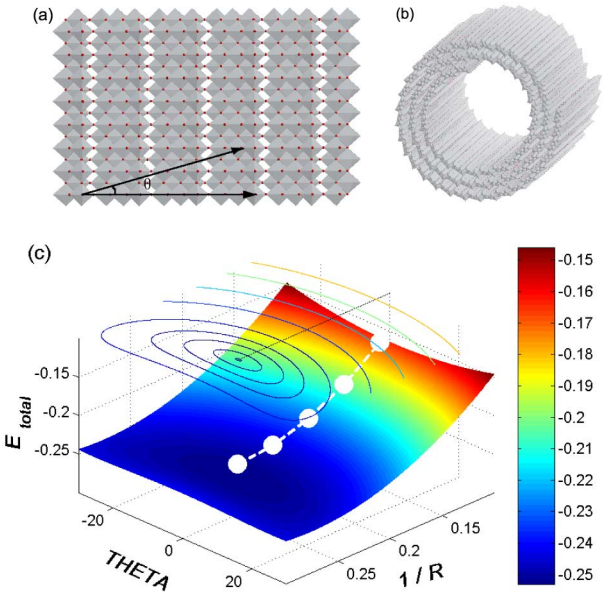

FIG. 4 (color online). (a) Structure model of a single trititanate sheet. (b) A nanotube formed by rolling the trititanate sheet along the [010] direction with a chiral vector along the [001] direction and a chiral angle $\theta = 0$. (c) Two-dimensional map of the total energy surface $E_{\text{total}}(\theta, R)$ as a function of the chiral angle θ and $1/R$.

nanotube R may be obtained by minimizing the total energy with respect to R giving $R = 4.3$ nm, and this value agrees well with our experimental observations. The dependence of the surface tension on the chiral angle comes into the equation because the surface tension due to the contraction of the relevant Ti-O bonds [lying on the (010) plane] may be most effectively released by rolling the trititanate layer along the [010] direction with $\theta = 0$ [Fig. 4(b)]. Shown in Fig. 4(c) is the $E_{\text{total}}(\theta, R)$ surface, and a path to the optimized geometry of the tube with $\theta = 0$, in a good agreement with experimental data.

For multiwall spiral nanotubes [7] additional factors need to be taken into account. On the one hand coupling between the shells of the multiwall nanotube can result in a large energy gain. On the other hand, the radius of curvature of the shells will deviate from the optimal curvature when the shell number increases. But the energy rise from the increase of the shell number is much smaller than the energy gain due to the shell coupling and, therefore, is not sufficient to terminate the rolling process. We noted that a hydrogen deficient $H_2Ti_3O_7$ crystal layer is negatively charged in solution, which results in a positive Coulomb repulsive energy E_{coulomb} when the negatively charged $H_{2-\delta}Ti_3O_7$ crystal layer rolls into a tube. The negative charge of the layer may be compensated partially by, e.g., the residual hydrogen ions H^+, oxygen vacancies and positively charged Na^+ ions on the inner and outer surfaces of the tube, and the uncompensated net charge inside the tube may result in a strong electrostatic Coulomb force to terminate the rolling process.

Shown in Fig. 5 are calculated shell coupling energy E_{coupl} and the electrostatic Coulomb energy E_{coulomb} as functions of the shell number [18]. For a nanotube with two or three shells E_{coupl} dominates the total energy, driving the rolling process to proceed. When the shell number increases E_{coulomb} increases rapidly and at about four shells E_{total} becomes positive and the rolling process stops. Experimentally it was found that the $H_2Ti_3O_7$-type nanotubes have typically four shells. Figure 5 shows that finite residual charges in the interlayer region may result in a narrow distribution of the shell number. It should be noted that the initial size of the crystal plates may also affect this distribution.

In summary, we proposed a new mechanism for the formation of trititanate nanotubes in the reaction of TiO_2 and NaOH. Crystalline TiO_2 decomposed into a disordered phase first, from which some $H_2Ti_3O_7$-type plates grow. Individual trititanate layers are peeled off from the plates and scroll up into nanotubes. It was found that surface tension due to an asymmetry related to H deficiency in the surface layers of the plates is the principal driving force of the cleavage and the dimension of the nanotubes is controlled by this surface tension together with interlayer coupling energy and Coulomb force. Our very recent synthesis of nanotubes directly from some layered trititanates supports this mechanism which, we believe, may also be applied to the formation of many other inorganic nanotubes.

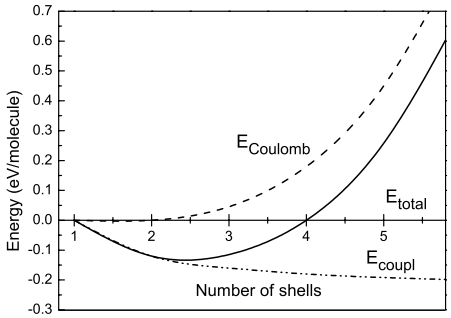

FIG. 5. Competing contributions of coupling energy and Coulomb energy to the total lattice energy as functions of the number of shells in a multiwall nanotube.

This work was supported by the Ministry of Science and Technology (001CB610502), National Science Foundation of China (90206021), Chinese Academy of Sciences, and Peking University.

*To whom correspondence should be addressed.
Email address: plm@ele.pku.edu.cn

[1] S. Iijima, Nature (London) **345**, 56 (1991).
[2] S. Amelinckx, X. B, Zhang, D. Bernaerts, X. F. Zhang, V. Ivanov, and J. B. Nagy, Science **265**, 635 (1994).
[3] R. Tenne and A. K. Zettl, in *Carbon Nanotubes–Synthesis, Structure, Properties and Applications*, edited by M. S. Dresselhaus, G. Dresselhaus, and P. Avouris (Springer, Berlin, 2001), p. 81.
[4] S. Sawada and N. Hamada, Solid State Commun. **83**, 917 (1992).
[5] O. G. Schmidt and K. Eberl, Nature (London) **410**, 168 (2001).
[6] L. Pauling, Proc. Natl. Acad. Sci. U.S.A. **16**, 578 (1930).
[7] Q. Chen, W. Zhou, G. H. Du, and L.-M. Peng, Adv. Mater. **14**, 1208 (2002).
[8] T. Kasuga, M. Hiramatsu, A. Hoson, T. Sekino, and K. T. Niihara, Adv. Mater. **11**, 1307 (1999).
[9] M. C. Payne *et al.*, Rev. Mod. Phys. **64**, 1045 (1992).
[10] Accelry, see http://www.accelrys.com (2002).
[11] D. Vanderbilt, Phys. Rev. B **41**, 7892 (1990).
[12] B. Hammer, L. B. Hansen, and J. K. Norskov, Phys. Rev. B **59**, 7413 (1999).
[13] H. J. Monkhorst and J. D. Pack, Phys. Rev. B **13**, 5188 (1976).
[14] J. K. Burdett *et al.*, J. Am. Chem. Soc. **109**, 3639 (1987).
[15] R. Asahi, Y. Taga, W. Mannstadt, and A. J. Freeman, Phys. Rev. B **61**, 7459 (2000).
[16] S. Andersson and A. D. Wadsley, Acta Crystallogr. **14**, 1245 (1961).
[17] T. P. Feist and P. K. Davis, J. Solid State Chem. **101**, 275 (1992).
[18] S. Zhang *et al.*, (unpublished).
[19] J. Harris, Phys. Rev. B **31**, 1770 (1985).
[20] S. J. Vosko, L. Wilk, and M. Nusair, Can. J. Phys. **58**, 1200 (1980).